[19] Le QT, Eulau SM, George TI, et al. Primary radiotherapy for localized orbital MALT lymphoma. Int J Radiat Oncol Biol Phys 2002;52:657–63.
[20] Fung CY, Tarbell NJ, Lucarelli MJ, et al. Ocular adnexal lymphoma: clinical behavior of distinct world health organization classification subtypes. Int J Radiat Oncol Biol Phys 2003;57:1382–91.
[21] Hasegawa M, Kojima M, Shioya M, et al. Treatment results of radiotherapy for malignant lymphoma of the orbit and histopathologic review according to the WHO classification. Int J Radiat Oncol Biol Phys 2003;57:172–6.
[22] Martinet S, Ozsahin M, Belkacemi Y, et al. Outcome and prognostic factor in orbital lymphoma: a rare cancer network study on 90 consecutive patients treated with radiotherapy. Int J Radiat Oncol Biol Phys 2003;55:892–8.
[23] Olivier KR, Brown PD, Stafford SL, et al. Efficacy and treatment-related toxicity of radiotherapy for early-stage primary non-Hodgkin lymphoma of the parotid gland. Int J Radiat Oncol Biol Phys 2004;60:1510–4.
[24] Zhou P, Ng AK, Silver B, et al. Radiation therapy for orbital Lymphoma. Int J Radiat Oncol Biol Phys 2005;3:66–871.
[25] Wenzel C, Fiebiger W, Dieckmann K, et al. Extranodal marginal zone B-cell lymphoma of mucosa-associated lymphoid tissue of the head and neck area. Cancer 2003;67:2236–41.
[26] Tsang RW, Gospodarowicz MK, Pintilie M, et al. Stages I and II MALT lymphoma: results of treatment with radiotherapy. Int J Radiat Oncol Biol Phys 2001;50:1258–64.
[27] Hitchcock S, Ng AK, Fisher DC, et al. Treatment outcome of mucosa-associated lymphoid tissue/marginal zone non-Hodgkin's lymphoma. Int J Radiat Oncol Biol Phys 2002;52:1058–66.
[28] Tsang RW, Gospodarowicz MK, Pintilie M, Wells W, Hodgson DC, Sun A, et al. Localized mucosa-associated lymphoid tissue lymphoma treated with radiation therapy has excellent outcome. J Clin Oncol 2003;21:4157–64.
[29] Schechter NR, Portlock CS, Yahalom J. Treatment of mucosa associated lymphoid tissue lymphoma of the stomach with radiation alone. J Clin Oncol 1998;16:1916–21.
[30] Fung CY, Grossbard ML, Linggood RM, et al. Mucosa-associated lymphoid tissue lymphoma of the stomach. Cancer 1999;85:9–17.
[31] Isobe K, Kagami Y, Higuchi K, Kodaira T, Hasegawa M, Shikama N, et al. Japan Radiation Oncology Group. A multicenter phase II study of local radiation therapy for stage IEA mucosa-associated lymphoid tissue lymphomas: a preliminary report from the Japan Radiation Oncology Group (JAROG). Int J Radiat Oncol Biol Phys 2007;69:1181–6.
[32] Allal A, Kurtz JM, Pipard G, Marti MC, Miralbell R, Popowski Y, et al. Chemoradiotherapy versus radiotherapy alone for anal cancer: a retrospective comparison. Int J Radiat Oncol Biol Phys 1993;27:59–66.
[33] Esik O, Ikeda H, Mukai K, Kaneko A. A retrospective analysis of different modalities for treatment of primary orbital non-Hodgkin's lymphomas. Radiother Oncol 1996;38:13–8.
[34] Sasai K, Yamabe H, Dodo Y, Kashii S, Nagata Y, Hiraoka M. Non-Hodgkin's lymphoma of the ocular adnexa. Acta Oncol 2001;40:485–90.
[35] Lee JL, Kim MK, Lee KH, Hyun MS, Chung HS, Kim DS, et al. Extranodal marginal zone B-cell lymphomas of mucosa-associated lymphoid tissue-type of the orbit and ocular adnexa. Ann Hematol 2005;84:13–8.
[36] Jäger G, Neumeister P, Brezinschek R, Hinterleitner T, Fiebiger W, Penz M, et al. Treatment of extranodal marginal zone B-cell lymphoma of mucosa-associated lymphoid tissue type with cladribine: a phase II study. J Clin Oncol 2002;20:3872–7.
[37] Zinzani PL, Stefoni V, Musuraca G, Tani M, Alinari L, Gabriele A, et al. Fludarabine-containing chemotherapy as frontline treatment of nongastrointestinal mucosa-associated lymphoid tissue lymphoma. Cancer 2004;100:2190–4.
[38] Taal BG, Burgers JM, van Heerde P, Hart AA, Somers R. The clinical spectrum and treatment of primary non-Hodgkin's lymphoma of the stomach. Ann Oncol 1993;4:839–46.
[39] Ruskoné-Fourmestraux A, Aegerter P, Delmer A, Brousse N, Galian A, Rambaud JC. Primary digestive tract lymphoma: a prospective multicentric study of 91 patients. Groupe d'Etude des Lymphomes Digestifs. Gastroenterology 1993;105:1662–71.
[40] Hammel P, Haioun C, Chaumette MT, Gaulard P, Divine M, Reyes F, et al. Efficacy of single-agent chemotherapy in low-grade B-cell mucosa-associated lymphoid tissue lymphoma with prominent gastric expression. J Clin Oncol 1995;13:2524–9.
[41] Conconi A, Martinelli G, Thiéblemont C, Ferreri AJ, Devizzi L, Peccatori F, et al. Clinical activity of rituximab in extranodal marginal zone B-cell lymphoma of MALT type. Blood 2003;102:2741–5.
[42] Martinelli G, Laszlo D, Ferreri AJ, Pruneri G, Ponzoni M, Conconi A, et al. Clinical activity of rituximab in gastric marginal zone non-Hodgkin's lymphoma resistant to or not eligible for anti-*Helicobacter pylori* therapy. J Clin Oncol 2005;23:1979–83.
[43] Zinzani PL, Magagnoli M, Galieni P, Martelli M, Poletti V, Zaja F, et al. Nongastrointestinal low-grade mucosa-associated lymphoid tissue lymphoma: analysis of 75 patients. J Clin Oncol 1999;17:1254–8.
[44] Arcaini L, Burcheri S, Rossi A, Passamonti F, Paulli M, Boveri E, et al. Nongastric marginal-zone B-cell MALT lymphoma: prognostic value of disease dissemination. Oncologist 2006;11:285–91.
[45] Zucca E, Conconi A, Pedrinis E, Cortelazzo S, Motta T, Gospodarowicz MK, et al. International Extranodal Lymphoma Study Group. Nongastric marginal zone B-cell lymphoma of mucosa-associated lymphoid tissue. Blood 2003;101:2489–95.
[46] Papaxoinis G, Fountzilas G, Rontogianni D, Dimopoulos MA, Pavlidis N, Tsatalas C, et al. Low-grade mucosa-associated lymphoid tissue lymphoma: a retrospective analysis of 97 patients by the Hellenic Cooperative Oncology Group (HeCOG). Ann Oncol 2007 Dec 20. Epub ahead of print.
[47] Conconi A, Bertoni F, Pedrinis E, Motta T, Roggero E, Luminari S, et al. Nodal marginal zone B-cell lymphomas may arise from different subsets of marginal zone B lymphocytes. Blood 2001;98:781–6.
[48] Jäger G, Neumeister P, Quehenberger F, Wöhrer S, Linkesch W, Raderer M. Prolonged clinical remission in patients with extranodal marginal zone B-cell lymphoma of the mucosa-associated lymphoid tissue type treated with cladribine: 6 year follow-up of a phase II trial. Ann Oncol 2006;17:1722–3.
[49] Pfeffer MR, Rabin T, Tsvang L, Goffman J, Rosen N, Symon Z. Orbital lymphoma: is it necessary to treat the entire orbit? Int J Radiat Oncol Biol Phys 2004;60:527–30.
[50] Terai S, Iijima K, Kato K, Dairaku N, Suzuki T, Yoshida M, et al. Long-term outcomes of gastric mucosa-associated lymphoid tissue lymphomas after *Helicobacter pylori* eradication therapy. Tohoku J Exp Med 2008;214:79–87.
[51] Suh CO, Shim SJ, Lee SW, Yang WI, Lee SY, Hahn JS. Orbital marginal zone B-cell lymphoma of MALT: radiotherapy results and clinical behavior. Int J Radiat Oncol Biol Phys 2006;65:228–33.
[52] Le QT, Eulau SM, George TI, Hildebrand R, Warnke RA, Donaldson SS, et al. Primary radiotherapy for localized orbital MALT lymphoma. Int J Radiat Oncol Biol Phys 2002;52:657–63.
[53] Zhou P, Ng AK, Silver B, Li S, Hua L, Mauch PM. Radiation therapy for orbital lymphoma. Int J Radiat Oncol Biol Phys 2005;63:866–71.

Jpn J Clin Oncol 2008;38(6)438–444
doi:10.1093/jjco/hyn038

Three-dimensional Conformal Radiotherapy for Hepatocellular Carcinoma with Inferior Vena Cava Invasion

Hiroshi Igaki[1], Keiichi Nakagawa[1], Kenshiro Shiraishi[1], Shuichiro Shiina[2], Norihiro Kokudo[3], Atsuro Terahara[1], Hideomi Yamashita[1], Nakashi Sasano[1], Masao Omata[2] and Kuni Ohtomo[1]

[1]Departments of Radiology, [2]Gastroenterology and [3]Hepato-Biliary-Pancreatic Surgery, The University of Tokyo Hospital, Tokyo, Japan

Received February 25, 2008; accepted April 24, 2008; published online May 21, 2008

Background: Hepatocellular carcinoma with inferior vena cava invasion is a rare but fatal condition of disease progression. The aim of this study was to analyze the results of treatment for hepatocellular carcinoma with inferior vena cava invasion by three-dimensional conformal radiation therapy.

Methods: From 1990 to 2006, 18 histopathologically confirmed hepatocellular carcinoma patients with inferior vena cava invasion who were unsuitable for surgery were treated by three-dimensional conformal radiation therapy at our hospital with two to four static or dynamic conformal arc fields.

Results: A median total tumor dose of 50 Gy (range 30–60 Gy) was delivered. The progression-free rate was 91.6% among the patients in whom follow-up computed tomography was obtained. Actuarial survival at 1 year was 33.3%, and the median survival period was 5.6 months.

Conclusions: Three-dimensional conformal radiation therapy might offer a chance of long survival for a part of the hepatocellular carcinoma patients with inferior vena cava invasion, since a third of such patients survived more than a year. Additional treatments should be considered to prevent distant metastases and hepatic functional deterioration after three-dimensional conformal radiation therapy.

Key words: hepatocellular carcinoma – inferior vena cava – three-dimensional conformal radiation therapy – hepatic functional reserve – liver cirrhosis

INTRODUCTION

Hepatocellular carcinoma (HCC) is the eighth major cause of cancer death in the United States and the third in Japan (1,2). Local ablative therapies such as hepatectomy, radiofrequency ablation (RFA) and percutaneous ethanol injection (PEI) should be administered, if possible, to patients with limited extension of HCC. But when the tumor invades the inferior vena cava (IVC), these treatments are indicated only for very few patients. In some reports, a part of these patients can survive long by hepatic resection combined with IVC resection (3–5). But such aggressive surgeries are not suitable for most patients, and other treatment modalities are also restricted not only by poor hepatic function, but also frequently by extensive disease progression. Transcatheter arterial chemoembolization (TACE) is often tried in HCC patients with IVC invasion for whom ablative treatment is unsuitable. However, TACE rarely achieves local tumor control to prolong survival periods sufficiently in such a critical condition, although the efficacy of this treatment has been proven in meta-analyses (6,7).

A few decades ago, liver was assumed to be a highly radiosensitive organ that was unsuitable for high-dose radiotherapy. But recent progress in radiation oncology has enabled us to concentrate high-dose radiation on liver tumors while preserving hepatic function after treatment (8–15). In addition, some institutions apply stereotactic radiotherapy to solitary small liver tumors. Consequently, radiotherapy has come to play an important role in multidisciplinary treatment of HCC.

At our institution, three-dimensional conformal radiation therapy (3D-CRT) has been the primary treatment strategy for HCC with portal vein invasion, and has achieved good clinical results (9). As with the treatment of HCC patients

For reprints and all correspondence: Hiroshi Igaki, Department of Radiology, The University of Tokyo Hospital, 7-3-1, Hongo, Bunkyo-ku, Tokyo 113-8655, Japan. E-mail: igaki-tky@umin.ac.jp

with portal vein invasion, radiotherapy is considered for HCC patients with IVC invasion at our institution if they are unsuitable for surgery. But there are few reports on radiotherapy for such patients (16), and the natural course of such conditions is not well known. In the present study, we retrospectively reviewed the medical records of HCC patients with IVC invasion and analyzed the efficacy of radiotherapy in these patients.

METHODS

From 1990 to 2006, 18 HCC patients with IVC invasion were treated by radiotherapy at our hospital. Their clinical courses and treatment results were retrospectively reviewed. HCC was diagnosed by using ultrasonography, computed tomography (CT), angiography and liver biopsy. In each patient, the diagnosis was confirmed histopathologically. IVC invasion was defined by a low-attenuation mass that protruded into the intraluminal space of IVC on enhanced CT and/or detection of pulsatile flow in IVC thrombi by Doppler ultrasonography. The patients' characteristics are shown in Table 1.

Patients with liver cirrhosis of Child–Pugh class C were not indicated for the treatment. CT-based radiotherapy treatment planning was made for all patients by the following treatment planning systems, RPS700U(3D) (Mitsubishi Electric Co., Tokyo, Japan) or Pinnacle[3] (Philips/ADAC, Milpitas, CA, USA). Clinical target volume was contoured on serial CT images with a 0.5–1-cm margin around the gross tumor volume, covering IVC-protruding tumor as well as the primary tumor invading to the IVC. Other co-existing intrahepatic tumors which had no continuity to the IVC-invading tumor were not included in the clinical target volume, and managed by other treatment modalities. Planning target volume was determined by a 0.5–2.0-cm margin around the clinical target volume. A dynamic conformal arc or two to four static ports were used for irradiation. In earlier periods, dynamic conformal arc therapy or multiport (mainly four ports) treatment plans were used, and we could not obtain dose-volume histograms in the treatment-planning machine. In recent years, treatment plans using two opposed fields have been preferred, because such treatment enables the maximization of the non-irradiated volume of the normal liver tissue. This treatment planning strategy is based on the fact that the normal liver tissue tolerance is lower in patients with viral hepatitis and liver cirrhosis than

Table 1. Patient characteristics

Case no.	Age and sex	Previous treatment				Etiology	Child–Pugh class	Pre-treatment AFP (ng/mL)[1]	Pre-treatment PIVKAII (mAu/mL)[2]
		Surgery	TACE	PEI	RFA				
1	48M	Information not available				HBV	A	38	1
2	67M	Information not available				HBV	B	60	8
3	63M	○		○		Unknown	A	9	N/A
4	67M			○		HCV	A	2385	125
5	80F	Information not available				HCV	A	3	1134
6	58M		○			Alcohol	B	9	26622
7	45M	○	○			HBV	B	136260	10784
8	71M		○		○	HCV	B	4	3242
9	74M		○			HCV	B	10	88
10	70M		○			HCV	B	13	7207
11	61M		○			HCV	B	21	3639
12	72M	○	○	○	○	HCV	A	6175	28
13	70M		○			HCV	B	126	39
14	76M		○			HCV	B	20	3572
15	71M	○	○			HCV	A	11	538
16	74M		○	○	○	HCV	A	38	681
17	69F		○		○	HCV	B	8	1119
18	81M	○	○	○	○	HCV	A	1	12008

Open circles indicate that the patient has received the specific treatment(s). M, male; F, female; TACE, transcatheter arterial chemoembolization; PEI, percutaneous ethanol injection; RFA, radiofrequency ablation; HBV, hepatitis B virus; HCV, hepatitis C virus; N/A, not available; PIVKAII, protein induced by Vitamin K absence-II.

[1]Normal range of serum concentration of AFP is <9 ng/mL.

[2]Normal range of serum concentration of PIVKAII is <40 mAu/mL.

in healthy patients (8). The general principle of treatment planning was to keep V_{30}, which was defined as the percent volume of the liver exceeding 30 Gy, lower than 30% of the whole liver volume minus tumor volume. We aimed for a total tumor dose of 50–60 Gy in conventional fractionation, but allowed smaller doses according to the dose-volume histogram of the normal liver at the physician's discretion. X-rays were delivered by linear accelerators ML15-MDX (Mitsubishi Electric Co., Tokyo, Japan) or CRS-6000 (Mitsubishi Electric Co., Tokyo, Japan). Written informed consent was obtained from the patients before treatment.

Follow-up and survival periods were calculated from the first day of radiation therapy. Actuarial survival rates were calculated by the Kaplan–Meier method. The statistical significance between groups was assessed with the log-rank test. Differences were considered statistically significant when $P < 0.05$.

RESULTS

All patients tolerated the treatment well. No severe complications were observed during the treatment period. The total tumor dose ranged from 30 to 60 Gy, with a median dose of 50 Gy (Table 2). All patients were followed until death except for the three patients who were alive at the time of analysis. Other treatment variables and results are summarized in Table 2.

Treatment response was defined as the tumor status at the last follow-up CT (Table 2). The response rate (complete response + partial response) and progression-free rate (complete response + partial response + stable disease) were 33.3% (95% confidential interval: 6.7–60.0%) and 91.6% (95% confidential interval: 75.9–100%), respectively, among the 12 patients for whom follow-up CTs were obtained. Only one patient developed local progression of the IVC-invading tumor within 6 months after 3D-CRT, and this was determined to be a progressive disease. This patient started systemic chemotherapy with 5-fluorouracil and interferon after diagnosis of a progressive disease, and was alive at the time of this analysis with no further progression of the tumor after introduction of this chemotherapy, 26.2 months after treatment. In the remaining 11 patients, no tumor regrowth was observed within the irradiated volume at the last follow-up.

At the time of the last follow-up, three patients were alive and the others were dead. Actuarial survival rate was 33.3% at 1 year, with a median survival period of 5.6 months (Fig. 1). The causes of death are shown in Table 2. The Child–Pugh class A group tended to survive longer than the class B group, but the difference did not reach statistical significance level (7.8 months versus 3.3 months, $P = 0.136$, Fig. 2 and Table 3). The survival period did not differ between responders (complete response + partial response) and non-responders (stable disease + progressive disease) (Fig. 3 and Table 3). Older patients (70 years or older) and

Table 2. Treatment-related variables and results

Case no.	Total dose (Gy)	Equivalent dose (Gy)[1]	Irradiation technique	Treatment response	Follow-up period (months)	Cause of death
1	48	52	Opposed two fields	N/A	5.6	Unknown
2	48	52	Dynamic conformal	N/A	3.0	Unknown
3	30	37.5	Dynamic conformal	N/A	7.2	Unknown
4	42	42	Dynamic conformal	N/A	1.3	Pulmonary metastasis
5	60	60	Dynamic conformal	CR	7.8	Non-tumoral Liver failure
6	50	50	Dynamic conformal	N/A	3.7	Rupture of esophageal varix
7	50	50	Four fields	SD	3.3	Tumor-related Liver failure
8	46	46	Four fields	SD	2.6	Non-tumoral Liver failure
9	50	50	Four fields	PR	7.2	Pulmonary metastasis
10	50	50	Dynamic conformal	PR	16.3	Non-tumoral Liver failure
11	40	40	Four fields	SD	1.8	Pulmonary metastasis
12	50	50	Dynamic conformal	CR	13.7	Tumor-related Liver failure
13	52	52	Four fields	N/A	1.6	Pulmonary embolization
14	46	46	Opposed two fields	SD	4.7	Tumor-related Liver failure
15	50	50	Four fields	SD	14.5	Brain metastasis
16	50	50	Non-coplanar	PD	26.2	(Alive)
17	40	40	Opposed two fields	SD	12.6	(Alive)
18	50	50	Opposed two fields	SD	10.2	(Alive)

CR, complete response; PR, partial response; SD, stable disease; PD, progressive disease.
[1]Equivalent dose in conventional fractionation of 2.0 Gy per fraction was calculated based on a linear quadratic model assuming $\alpha/\beta = 10$ (32).

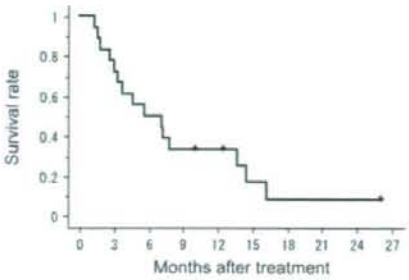

Figure 1. Overall survival of the whole group of 18 patients.

patients with hepatitis C virus tended to survive longer than the other patients, but the differences were also not statistically significant (Fig. 4). The median survival periods were 7.8 and 3.3 months for the groups 70 years or older and under 70 years, respectively ($P = 0.064$). The median survival periods of the patients with HCV carriers and other etiologies were 7.8 and 3.7 months, respectively ($P = 0.111$). A representative case is shown in Fig. 5.

Table 3. Univariate analysis of potential prognostic factors

Factor	*n*	Median survival (months)	*P* value
Etiology			
HCV	13	7.8	0.111
Others	5	3.7	
Treatment response			
Responders	4	7.8	0.894
Non-responders	8	4.6	
Age at treatment			
≥ 70	10	7.8	0.064
< 70	8	3.3	
Child–Pugh class			
A	8	7.8	0.136
B	10	3.3	
Pre-treatment AFP			
≤ 20 ng/mL	10	7.2	0.305
> 20 ng/mL	8	3.0	
Pre-treatment PIVKA II			
≤ 1000 mAu/mL	9	5.6	0.987
> 1000 mAu/mL	9	4.7	

DISCUSSION

HCC with IVC invasion is difficult to treat and associated with poor prognosis, because of its inherent nature of serious condition of the disease and the limited availability of treatment strategies. We have treated such patients by 3D-CRT, and here reviewed their treatment results retrospectively.

The literature offers no detailed data on the natural history of HCC with IVC invasion. But vascular invasion from HCC has been associated with miserable prognoses (16–18) and a limited life expectancy of 2–3 months, if untreated. However, Mizumoto et al. (19) reported good clinical results of proton beam therapy in patients with HCC invading to the IVC. All three of the patients they treated lived more than a year after this therapy.

The prognosis of patients with HCC is known to be dependent on the hepatic functional reserve (20,21). Our results are consistent with this knowledge, because the median survival of Child–Pugh class A patients was slightly longer than that of class B patients (Fig. 2). On the other hand, treatment response did not influence patients' survival periods (Fig. 3). But the treatment response after radiotherapy is predictive of survival in the curative treatment settings in many primary cancer sites (22–24). There are three possible explanations for this: (i) a relatively long period (typically several months) is required for tumor shrinkage after radiotherapy, considering the median survival periods of these patients; (ii) fatal deterioration of hepatic function can be seen, owing to the damage to normal liver tissue as a result of radiotherapy; (iii) it is sometimes difficult to distinguish the tumor thrombus from blood clots adhering to the IVC-invading tumor on follow-up CT images; and (iv) the group in this analysis was too small for statistical differences. Older age was a marginally significant prognostic factor in our results (Fig. 4). Age as a prognostic factor,

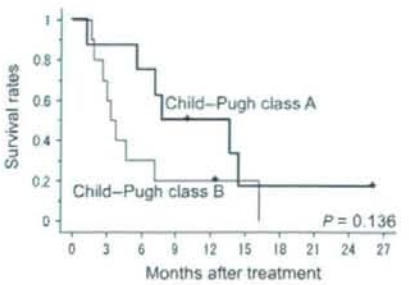

Figure 2. Overall survival by pre-treatment hepatic functional reserve.

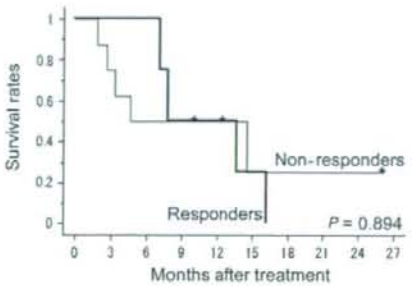

Figure 3. Overall survival by treatment response.

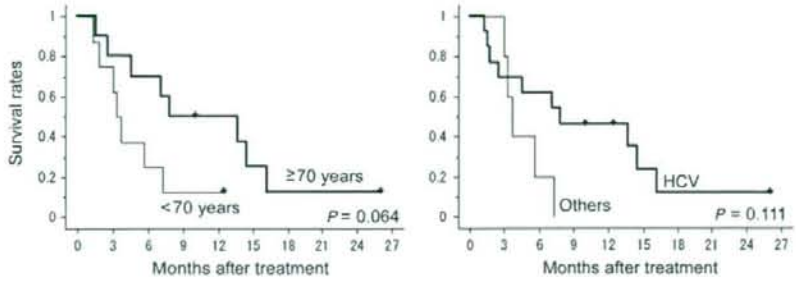

Figure 4. Overall survival by age (left panel) or etiology (right panel).

however, is controversial in the literature, because older age might sometimes be a favorable prognostic factor in some conditions but an unfavorable one in others (25–27).

In our experience, six patients died of liver failure. Of these six, three were assumed to be owing to the intrahepatic tumor growth from their clinical courses, and the other three were brought by undetermined causes. We could not differentiate the natural course of cirrhosis from treatment-related liver failure exactly. In this respect, we could not exclude the possibility of the treatment-related morbidities in Cases 5, 8 and 10 in Tables 1 and 2 with liver failures, although there had been no case with clinically apparent radiation-induced liver disease (RILD). In addition, there is no denying that the rupture of esophageal varix and the pulmonary embolization have occurred irrelevant to 3D-CRT or other treatments in Cases 6 and 13. But after 3D-CRT, 33.3% of our patients survived more than a year. In this respect, our 3D-CRT appeared to offer a chance to survive more than a year for a third of the patients with such critical conditions, although the median survival period was not satisfactory. The reason for such unsatisfactory results included the high incidence of deaths due to metastatic disease or liver failure despite the good progression-free rate of 91.6% for the irradiated IVC-invading tumor.

To minimize the probability of radiotherapy-related liver failure, treatment strategies have been improved (28,29). Despite these efforts, RILD can sometimes occur typically 2 weeks to 4 months after hepatic irradiation, and the threshold for RILD is reported to be 31 Gy of mean liver dose (29). Moreover, 50–76% of the patients who developed RILD died of this complication (30,31). Considering these situations, 3D-CRT has a potential benefit over the conventional two-dimensional radiotherapy in the viewpoint of normal liver protection. This point, however, has not been demonstrated in the previous literature to the best of our knowledge.

Some institutions adopt stereotactic body radiotherapy by multi-port irradiation technique. But the volume of low-dose-irradiated normal liver tissue is increased by the multi-port irradiation, especially when the clinical target volume is large. Radiation tolerance of the non-cancerous liver with chronic viral hepatitis or cirrhosis is known to be lower than that of healthy liver (29). We have a hypothesis that two opposed fields radiotherapy might be more protective than multiple-port radiotherapy for the cirrhotic liver. This is why we changed the 3D-CRT strategy from multiple-port irradiation to two opposed fields irradiation. We are now under investigation of the effect of treatment strategy on the survival or on the risk of RILD.

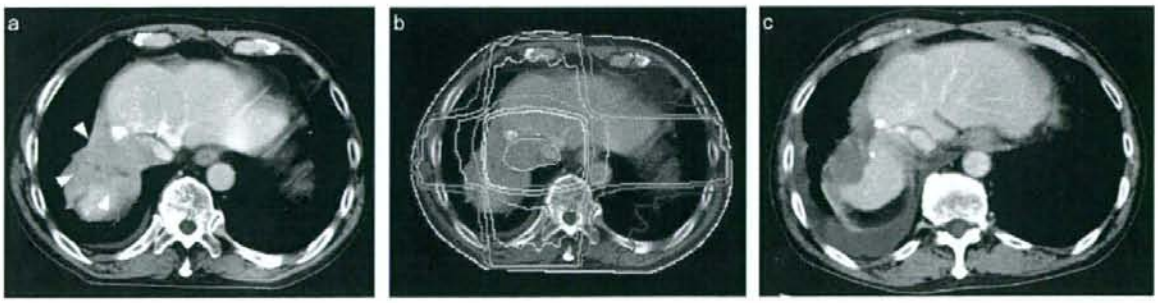

Figure 5. A representative case of a 72-year-old male with Child–Pugh class A hepatic function (case 12 in the Tables 1 and 2). (a) Before radiotherapy, the tumor located in S7 extended to IVC and the intraluminal space was narrow in the CT images. The tumor was indicated by the red arrowhead. (b) Dose distribution of the treatment plan. A total tumor dose of 50 Gy was delivered in 25 fractions by a dynamic conformal arc with four static fields. (c) Three months after radiotherapy. S7 tumor disappeared and no enhancement defect was observed within IVC, and the treatment response was judged as a complete response. The patient died of hepatic failure 13.7 months after irradiation. The irradiated tumor had no sign of regrowth at the time of death. (A colour version of this figure is available as supplementary data at http://www.jjco.oxfordjournals.org.)

Follow-up CT could not be obtained for six patients. This might be attributable in part to early deterioration in performance status, since all six died within 8 months after treatment. It is possible that disease control was not achieved in these patients and that the progression-free rate of 91.6% was thus overestimated. In this respect, additional treatments should be considered as many patients developed distant metastases or hepatic functional deterioration shortly after 3D-CRT.

CONCLUSIONS

A part of the HCC patients with IVC invasion might have benefited from 3D-CRT and a third of such patients had had a chance of surviving more than a year; otherwise they could not have survived long with this progressive fatal disease. However, further treatment should be considered to prevent distant metastasis and to protect post-treatment hepatic function, because the majority of the patients died from metastatic diseases or liver failure in spite of good local tumor control by 3D-CRT.

Funding

This work was supported by grants-in-aid for scientific research from the Ministry of Education, Science, and Culture of Japan (18790877 to H.I.).

Conflict of interest statement

None declared.

References

1. Surveillance Epidemiology and End Results NCI, US National Institute of Health [homepage on the Internet]. Summary of changes in cancer mortality, 1950–2004 and 5-year relative survival rates, 1950–2003 [cited 2008 February 26]. Available format: http://seer.cancer.gov/csr/1975_2004/results_single/sect_01_table.03.pdf.
2. Center for Cancer Control and Information Services, National Cancer Center, Japan [homepage on the Internet]. Graph database, Cancer information service for medical staff [cited 2008 February 26]. Available at: http://ganjoho.ncc.go.jp/pro/statistics/en/graph_db_index.html.
3. Arii S, Teramoto K, Kawamura T, Takamatsu S, Sato E, Nakamura N, et al. Significance of hepatic resection combined with inferior vena cava resection and its reconstruction with expanded polytetrafluoroethylene for treatment of liver tumors. *J Am Coll Surg* 2003;196:243–9.
4. Sarmiento JM, Bower TC, Cherry KJ, Farnell MB, Nagorney DM. Is combined partial hepatectomy with segmental resection of inferior vena cava justified for malignancy? *Arch Surg* 2003;138:624–30; discussion 630–1.
5. Hemming AW, Reed AI, Langham MR, Jr, Fujita S, Howard RJ. Combined resection of the liver and inferior vena cava for hepatic malignancy. *Ann Surg* 2004;239:712–9; discussion 719–21.
6. Cammà C, Schepis F, Orlando A, Albanese M, Shahied L, Trevisani F, et al. Transarterial chemoembolization for unresectable hepatocellular carcinoma: meta-analysis of randomized controlled trials. *Radiology* 2002;224:47–54.
7. Llovet JM, Bruix J. Systematic review of randomized trials for unresectable hepatocellular carcinoma: chemoembolization improves survival. *Hepatology* 2003;37:429–42.
8. Dawson LA, Ten Haken RK. Partial volume tolerance of the liver to radiation. *Semin Radiat Oncol* 2005;15:279–83.
9. Nakagawa K, Yamashita H, Shiraishi K, Nakamura N, Tago M, Igaki H, et al. Radiation therapy for portal venous invasion by hepatocellular carcinoma. *World J Gastroenterol* 2005;11:7237–41.
10. Huang CJ, Lian SL, Chen SC, Wu DK, Wei SY, Huang MY, et al. External beam radiation therapy for inoperable hepatocellular carcinoma with portal vein thrombosis. *Kaohsiung J Med Sci* 2001;17:610–4.
11. Tazawa J, Maeda M, Sakai Y, Yamane M, Ohbayashi H, Kakinuma S, et al. Radiation therapy in combination with transcatheter arterial chemoembolization for hepatocellular carcinoma with extensive portal vein involvement. *J Gastroenterol Hepatol* 2001;16:660–5.
12. Ishikura S, Ogino T, Furuse J, Satake M, Baba S, Kawashima M, et al. Radiotherapy after transcatheter arterial chemoembolization for patients with hepatocellular carcinoma and portal vein tumor thrombus. *Am J Clin Oncol* 2002;25:189–93.
13. Yamada K, Izaki K, Sugimoto K, Mayahara H, Morita Y, Yoden E, et al. Prospective trial of combined transcatheter arterial chemoembolization and three-dimensional conformal radiotherapy for portal vein tumor thrombus in patients with unresectable hepatocellular carcinoma. *Int J Radiat Oncol Biol Phys* 2003;57:113–9.
14. Kim DY, Park W, Lim DH, Lee JH, Yoo BC, Paik SW, et al. Three-dimensional conformal radiotherapy for portal vein thrombosis of hepatocellular carcinoma. *Cancer* 2005;103:2419–26.
15. Lin CS, Jen YM, Chiu SY, Hwang JM, Chao HL, Lin HY, et al. Treatment of portal vein tumor thrombosis of hepatoma patients with either stereotactic radiotherapy or three-dimensional conformal radiotherapy. *Jpn J Clin Oncol* 2006;36:212–7.
16. Zeng ZC, Fan J, Tang ZY, Zhou J, Qin LX, Wang JH, et al. A comparison of treatment combinations with and without radiotherapy for hepatocellular carcinoma with portal vein and/or inferior vena cava tumor thrombus. *Int J Radiat Oncol Biol Phys* 2005;61:432–43.
17. Llovet JM, Bustamante J, Castells A, Vilana R, Ayuso Mdel C, Sala M, et al. Natural history of untreated nonsurgical hepatocellular carcinoma: rationale for the design and evaluation of therapeutic trials. *Hepatology* 1999;29:62–7.
18. The Cancer of the Liver Italian Program (CLIP) Investigators. A new prognostic system for hepatocellular carcinoma: a retrospective study of 435 patients. *Hepatology* 1998;28:751–5.
19. Mizumoto M, Tokuuye K, Sugahara S, Hata M, Fukumitsu N, Hashimoto T, et al. Proton beam therapy for hepatocellular carcinoma with inferior vena cava tumor thrombus: report of three cases. *Jpn J Clin Oncol* 2007;37:459–62.
20. Franco D, Capussotti L, Smadja C, Bouzari H, Meakins J, Kemeny F, et al. Resection of hepatocellular carcinomas: results in 72 European patients with cirrhosis. *Gastroenterology* 1990;98:733–8.
21. Okuda K. Natural history of hepatocellular carcinoma including fibrolamellar and hepato-cholangiocarcinoma variants. *J Gastroenterol Hepatol* 2002;17:401–5.
22. Chen CH, Chang TT, Cheng KS, Su WW, Yang SS, Lin HH, et al. Do young hepatocellular carcinoma patients have worse prognosis? The paradox of age as a prognostic factor in the survival of hepatocellular carcinoma patients. *Liver Int* 2006;26:766–73.
23. Liem MS, Poon RT, Lo CM, Tso WK, Fan ST. Outcome of transarterial chemoembolization in patients with inoperable hepatocellular carcinoma eligible for radiofrequency ablation. *World J Gastroenterol* 2005;11:4465–71.
24. Wu DH, Liu L, Chen LH. Therapeutic effects and prognostic factors in three-dimensional conformal radiotherapy combined with transcatheter arterial chemoembolization for hepatocellular carcinoma. *World J Gastroenterol* 2004;10:2184–9.
25. Kayama T, Kumabe T, Tominaga T, Yoshimoto T. Prognostic value of complete response after the initial treatment for malignant astrocytoma. *Neurol Res* 1996;18:321–4.
26. Willers H, Wurschmidt F, Bunemann H, Heilmann HP. High-dose radiation therapy alone for inoperable non-small cell lung cancer—experience with prolonged overall treatment times. *Acta Oncol* 1998;37:101–5.
27. Kostakoglu L, Goldsmith SJ. PET in the assessment of therapy response in patients with carcinoma of the head and neck and of the esophagus. *J Nucl Med* 2004;45:56–68.
28. Lawrence TS, Robertson JM, Anscher MS, Jirtle RL, Ensminger WD, Fajardo LF. Hepatic toxicity resulting from cancer treatment. *Int J Radiat Oncol Biol Phys* 1995;31:1237–48.

29. Dawson LA, Normolle D, Balter JM, McGinn CJ, Lawrence TS, Ten Haken RK. Analysis of radiation-induced liver disease using the Lyman NTCP model. *Int J Radiat Oncol Biol Phys* 2002;53:810–21.
30. Cheng JC, Wu JK, Huang CM, Liu HS, Huang DY, Cheng SH, et al. Radiation-induced liver disease after three-dimensional conformal radiotherapy for patients with hepatocellular carcinoma: dosimetric analysis and implication. *Int J Radiat Oncol Biol Phys* 2002;54: 156–62.
31. Xu ZY, Liang SX, Zhu J, Zhu XD, Zhao JD, Lu HJ, et al. Prediction of radiation-induced liver disease by Lyman normal-tissue complication probability model in three-dimensional conformal radiation therapy for primary liver carcinoma. *Int J Radiat Oncol Biol Phys* 2006;65: 189–95.
32. Fowler JF. The linear–quadratic formula and progress in fractionated radiotherapy. *Br J Radiol* 1989;62:679–94.

hScrib, a human homologue of *Drosophila* neoplastic tumor suppressor, is a novel death substrate targeted by caspase during the process of apoptosis

Kenbun Sone[1], Shunsuke Nakagawa[1,*], Keiichi Nakagawa[2], Shin Takizawa[1], Yoko Matsumoto[1], Kazunori Nagasaka[1], Tetsushi Tsuruga[1], Haruko Hiraike[1], Osamu Hiraike-Wada[1], Yuichiro Miyamoto[1], Katsutoshi Oda[1], Toshiharu Yasugi[1], Koji Kugu[1], Tetsu Yano[1] and Yuji Taketani[1]

[1]*Department of Obstetrics and Gynecology, and*
[2]*Department of Radiology, Graduate School of Medicine, The University of Tokyo, 7-3-1 Hongo, Bunkyo-ku, Tokyo 113-8655, Japan*

hScrib, human homologue of *Drosophila* neoplastic tumor suppressor, was identified as a target of human papillomavirus E6 oncoprotein for the ubiquitin-mediated degradation. Here, we report that hScrib is a novel death substrate targeted by caspase. Full-length hScrib was cleaved by caspase during death ligands-induced apoptosis, which generates a p170 C-terminal fragments in Hela cells. *In vitro* cleavage assay using recombinant caspases showed that hScrib is cleaved by the executioner caspases. DNA damage-induced apoptosis caused loss of expression of full-length hScrib, which was recovered by addition of capase-3 inhibitor in HaCat cells. TUNEL positive apoptotic cells, which were identified 4 h after UV irradiation in HaCat cells, showed loss of hScrib expression at the adherens junction. Mutational analysis identified the caspase-dependent cleavage site of hScrib at the position of Asp-504. Although MDCK cells transfected with GFP-fused wild-type hScrib showed loss of E-cadherin expression and shrinkage of cytoplasm by UV irradiation, cells transfected with hScrib with Ala substitution of Asp-504 showed resistance to caspase-dependent cleavage of hScrib and intact expression of E-cadherin. These results indicate that caspase-dependent cleavage of hScrib is a critical step for detachment of cell contact during the process of apoptosis.

Introduction

Programmed cell death and morphological apoptosis is an intrinsic mechanism of self-destruction of cells (Steller 1995). Well-defined programmed cell death mechanism is crucial for successful embryogenesis and organogenesis (Jacobson *et al.* 1997). Disturbance of the apoptotic functions, which govern homeostasis of tissues, causes proliferation of overgrowing cells and leads to the tumor formation. The apoptotic surveillance mechanism usually causes fragmentation of chromosome and elimination of uncontrolled over-proliferated cells. Cancer cells are considered to develop by escaping from the cellular surveillance mechanisms governing tissue homeostasis. We previously identified hScrib as a target protein of high-risk human papillomavirus (HPV) E6 oncoprotein, which is considered to have a causal role in development of cervical cancer, for the ubiquitin-mediated degradation (Nakagawa & Huibregtse 2000). hScrib is shown to regulate cell cycle progression depending on its association with tumor suppressor protein adenomatous polyposis coli (APC) (Nagasaka *et al.* 2006; Takizawa *et al.* 2006). *Drosophila* Scribble localizes at the septate junction, which is functionally identical to the mammalian tight junction (Bilder & Perrimon 2000). hScrib localizes at the adherens junction in the epithelial MDCK cells (Nakagawa *et al.* 2004). Cysteine proteases from caspase family, which cleave their target proteins exclusively after the Asp residue, have an important function in the process of apoptosis (Brancolini *et al.* 1997; Nicholson & Thornberry 1997; Salvesen & Dixit 1997). Many proteins localized at the adherens junction are targeted by caspase for their cleavage. For instance, β-catenin (Brancolini *et al.* 1997), E-cadherin, plakoglobin, focal adhesion kinase (Levkau *et al.* 1998) and human Discs large (hDlg) (Gregorc *et al.*

Communicated by: Tadashi Yamamoto
**Correspondence:* Email: nakagawas-tky@umin.ac.jp

DOI: 10.1111/j.1365-2443.2008.01204.x

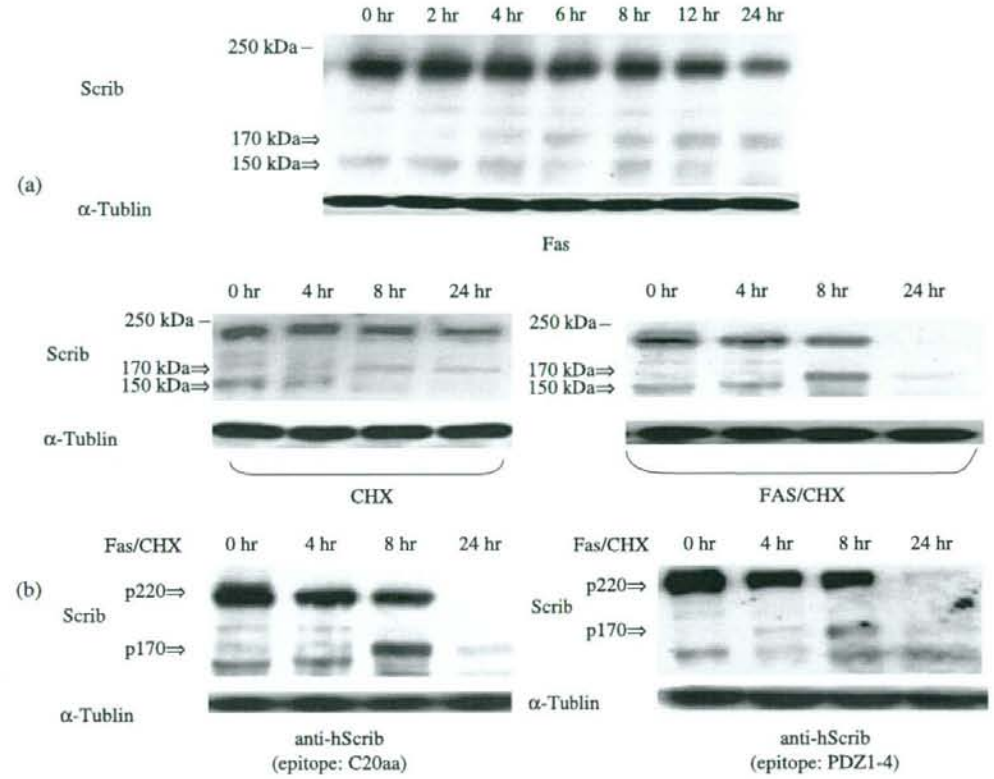

Figure 1 Cleavage of hScrib in Hela cells during Fas ligand-induced apoptosis. (a) HeLa cells were treated with Fas, CHX alone or Fas–CHX. Samples were taken at the times indicated. Western blotting as described in the Material and methods section monitored the amount of hScrib. The expression α-Tublin was shown as the internal control for each lane. (b) The cleavage of hScrib during apoptosis induced by Fas–CHX was analyzed by Western blotting with two antibodies raised against two different hScrib antigens. Note that p220 and p170 hScrib were detected by both of two antibodies. (Correction added after online publication 30 May 2008: This is the corrected version of Figure 1.)

2005) are cleaved by caspase during the process of apoptosis. Here, we identified that hScrib is targeted by caspase for cleavage during the process of apoptosis induced by death ligands and DNA damages.

Results

hScrib is cleaved during the process of apoptosis induced by death ligands and DNA damage

hScrib was shown to be cleaved and generate p170 hScrib during the process of apoptosis induced by death ligand, Fas (Fig. 1a). The band of full-length hScrib p220 and that of p170 generated by induction of apoptosis with Fas ligand and Cycloheximide (CHX) were identified by the two anti-hScrib antibodies raised against different epitopes (Fig. 1b). These data indicate that the full-length hScrib (p220) was cleaved during apoptosis and p170 hScrib was the cleaved product of full-length hScrib. There is one additional band in the lane of 0 h (p150, Figs 1, 2), which also disappeared by Fas–CHX or TNF–CHX treatment. This endogenous p150 was also identified by immunoblotting analysis with two anti-hScrib antibodies (Fig. 1b). The origin of p150 hScrib is currently unknown. The addition of CHX augmented cleavage of hScrib by the induction of apoptosis induced by Fas ligand (Fig. 1a). The hScrib p220 was completely disappeared 24 h after Fas–CHX or TNF–CHX treatment (Figs 1, 2). These data indicate that apoptosis activation by Fas ligand or TNF requires coordinate inhibition of

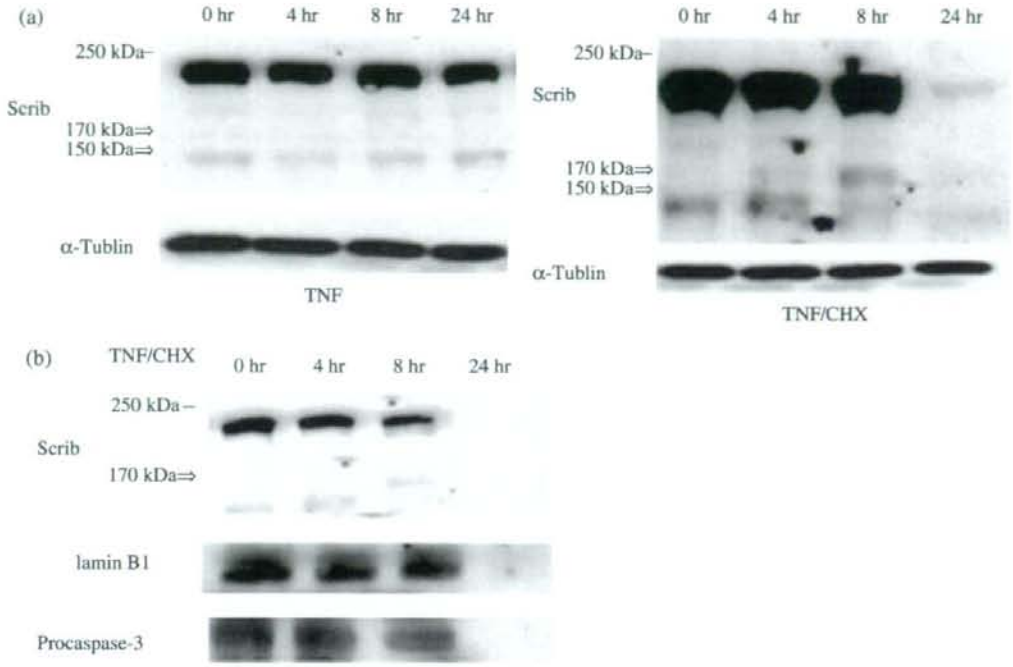

Figure 2 Cleavage of hScrib in Hela cells during TNF-induced apoptosis. (a) HeLa cells were treated with TNF alone or TNF–CHX. Samples were taken at the times indicated and the amount of hScrib was monitored by Western blotting. (b) The efficiency of cleavage of hScrib by the TNF–CHX treatment was compared with that of Lamin B1 or procaspase-3. The efficiency of cleavage of hScrib during apoptosis induced by UV irradiation was equivalent to that of Lamin B1 or procaspase-3. (Correction added after online publication 30 May 2008: This is the corrected version of Figure 2.)

survival signal that inhibit generation of prosurvival factors mediated by NF-κB (Perez & White 2000; Kucharczak *et al.* 2003). The cleavage of hScrib and generation of p170 hScrib were not observed by only TNF ligand, but by the combination of TNF ligand with CHX (Fig. 2a). We compared the efficiency of cleavage of hScrib by the TNF–CHX treatment with that of Lamin B1 or procaspase-3, which are reported to be the early targets for cleavage by caspase during apoptosis (Samejima *et al.* 1999). The efficiency of cleavage of hScrib during apoptosis induced by UV irradiation was equivalent to that of Lamin B1 or procaspase-3 (Fig. 2b).

hScrib localizes at the adherens junction in normal cells as previously reported (Fig. 3a) (Nakagawa *et al.* 2004). DNA damage by UV irradiation caused loss of expression of hScrib at the adherens junction in the apoptotic cells showing condensed (Fig. 3, arrow) or fragmented (Fig. 3, arrow head) nucleus showed by the Hoechst staining.

Loss of expression of hScrib is an early event during apoptosis-induced DNA damage

UV irradiation induced progressive decrease of hScrib expression at the cellular membrane along with time after UV irradiation (Fig. 4). Loss of hScrib expression was identified in the TUNEL positive cells after 4 h of UV irradiation (Fig. 4 UV4 h, arrow indicates TUNEL positive cells, which lost membrane bound expression of hScrib). These data suggest the possibility that hScrib in involved in the cellular detachment at the adherens junction in the early stage of apoptosis. The involvement of hDlg in elimination of apoptotic cell from cellular contact with normal cells, has been reported (Gregorc *et al.* 2005). We analyzed loss of expression of these tumor suppressors in Caco-2 cells, as these tumor suppressors are human homologues of *Drosophila* neoplastic tumor suppressors, in which mutation causes loss of tissue architecture and overgrowth of epithelial cells (Bilder &

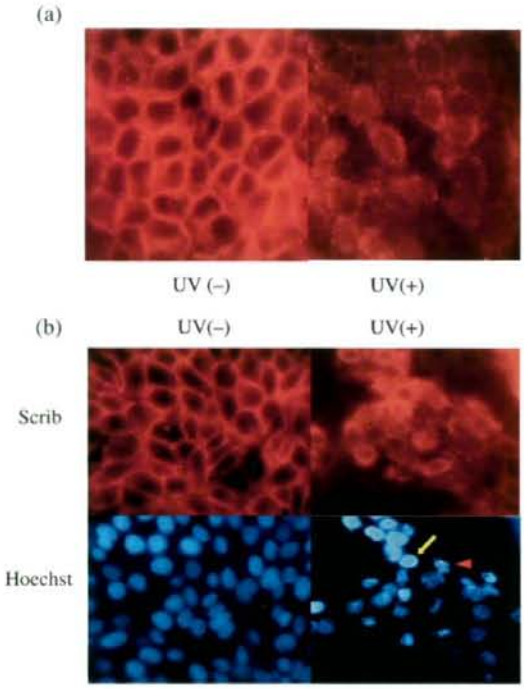

Figure 3 Loss of hScrib expression by the apoptosis induced by UV irradiation in HaCaT cells. (a) Apoptosis was induced with UV irradiation as described in the Materials and methods. Immunofluorescence images with anti-hScrib antibody were taken under the confocal microscopy before and after 6 h of UV irradiation. (b) Loss of hScrib expression at the cellular membrane was observed in the apoptotic cells showing condensed (arrow) or fragmented (arrow head) nucleus showed by the Hoechst staining.

Perrimon 2000). As shown in Fig. 5, the expressed level of hDlg in Caco-2 cells 8 h after UV irradiation was almost equivalent to that of untreated cells (Fig. 5a). In contrast, expression of hScrib was almost diminished in cells after 8 h of UV irradiation (Fig. 5a). Immunofluorescence analysis showed that the membrane-bound expression of hScrib was not observed, and it showed that dot-like expression, whereas hDlg still showed the membrane-bound expression in cells after 6 h of UV irradiation (Fig. 5b). At 12 h after irradiation of UV, expression of hScrib was not observed, but hDlg showed still faint but membrane-associated expression (Fig. 5b). These results indicate that hSrib is targeted by proteolysis earlier than the hDlg in apoptotic cells induced by UV irradiation.

hScrib is cleaved by the executioner caspases *in vitro*

Based on data described above, we investigated the possibility that hScrib is targeted for cleavage by caspase. *In vitro* translated hScrib was incubated with recombinant caspase-3, caspase-6, caspase-7 or caspase-8. hScrib was cleaved *in vitro* by the executioner caspases, caspase-3, caspase-6 and caspase-7 (Fig. 6a). The *in vitro* cleavage of hScrib by caspase-3 was completely repressed by the caspase-3 inhibitor (Fig. 6b). These data indicate that hScrib is a novel death substrate targeted by the executioner caspases.

hScrib is targeted by executioner caspase for proteolysis during the process of apoptosis

Next, we investigated the possibility that hScrib is targeted for cleavage by caspase *in vivo* during apoptosis. Apoptosis induced by UV irradiation caused cleavage of hScrib as mentioned above (Fig. 7). Loss of expression of hScrib as a result of cleavage by caspase activated with UV irradiation was recovered by addition of the caspase-3 inhibitor in the medium (Fig. 7). The caspase-6 inhibitor also showed the repressive effect on the cleavage of hScrib during apoptosis, but its inhibitory effect was weaker than that of caspase-3 inhibitor (Fig. 7). These data indicate that hScrib is targeted for cleavage during the process of apoptosis mainly by caspase-3.

504 Asp of hScrib is critical for caspase-dependent cleavage

Asp-X-X-Asp is reported to be conserved motif for caspase-dependent cleavage (Nicholson & Thornberry 1997; Talanian *et al.* 1997). There are two putative caspase-dependent cleave sites with amino acids Asp-X-X-Asp at 1068 Asp-X-X-1071 Asp and at 1131 Asp-X-X-1134 in amino acids sequence of hScrib. Alanine substitution of these Asp amino acids did not allow hScrib to resist to caspase-dependent cleavage (data not shown). hScrib consists of 16 canonical Leucine rich repeats (LRRs), LAP specific domain-a (LAPSD-a), LAPSD-b and four PDZ domains. We investigated which domains of hScrib are susceptible for cleavage by caspase *in vitro* by using several hScrib C-terminal deletion mutants. Human Scrib mutants, LRR–PDZ3, LRR–PDZ2 and LRR–PDZ1 were cleaved by recombinant caspase-3, whereas LRR–LAPSD and LRR were not susceptible for cleavage. These data indicate that hScrib is cleaved by caspase-3 at the C-terminal region of LAPSD (Fig. 8a). Mutational analysis found that Ala substitution of Asp 504 allows hScrib to resist to caspase-3 dependent cleavage (Fig. 8b).

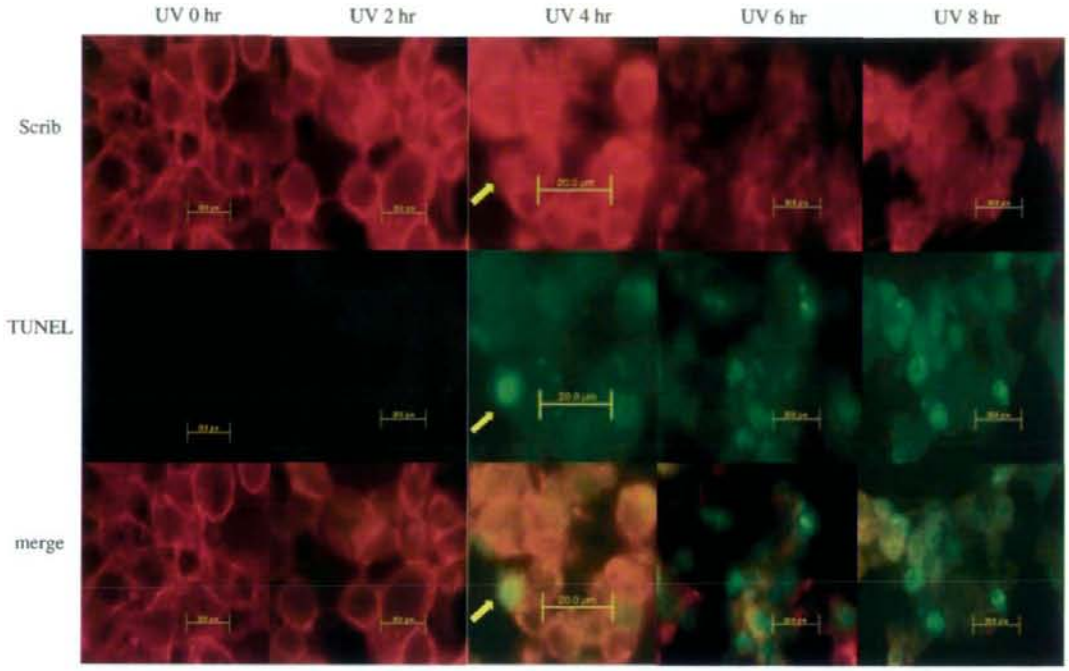

Figure 4 Loss of hScrib expression is an early event during apoptotic process. Cells irradiated with UV were analyzed by immunofluorescence staining with anti-hScrib antibody and TUNEL at the indicated time after UV irradiation. Note that hScrib expression was lost in the TUNEL positive cell (UV 4 h). The arrow indicates that loss of hScrib expression is observed in the TUNEL positive cells after 4 h of UV irradiation.

Alanine substitution of Asp 526 resided at the C-terminus of the LAPD of hScrib did not render hScrib resistant to caspase-3 dependent cleavage (Fig. 8b).

hScrib with Ala substitution of Asp 504 is resistant to caspase-dependent cleavage during the process of apoptosis induced by UV irradiation

GFP-tagged wild-type hScrib transfected MDCK cells showed loss of E-cadherin and hScrib expression at the membrane, fragmentation of nucleus and shrinkage of cytoplasm by apoptosis induction with UV irradiation (Fig. 9a,b). In contrast, GFP-tagged Asp504Ala hScrib mutant transfected MDCK cells showed the intact expression of transfected hScrib and E-cadherin, despite of fragmentation of nucleus showed by the Hoechst staining (Fig. 9c,d). Immunoblotting analysis confirmed that over-expressed GFP–hScrib D504A mutant is resistant to caspase-dependent cleavage activated by apoptosis induction with UV irradiation (Fig. 10a). To quantify the effect of WT and Asp504Ala hScrib mutant on apoptosis induction and cellular detachment, 300 MDCK cells transfected with control vector, GFP–WT hScrib vector, or GFP–hScrib D504A mutant vector were analyzed for apoptosis signals and cellular detachment by Hoechst staining and immunofluorescence analysis of E-cadherin, respectively (Fig. 10b). UV irradiation induced apoptosis and cellular detachment approximately in 80% MDCK cells transfected with control vector or GFP–WT hScrib vector. Although apoptosis was observed over 80% of cells transfected with GFP–hScrib D504A mutant vector, cellular detachment was only observed in 9% of those cells. These data indicate that caspase-dependent cleavage of hScrib has a crucial role in cellular detachment during progression of apoptosis.

Effect of HPV E6 expression on the caspase-dependent cleavage of hScrib during apoptosis

We investigated whether E6 expression have an effect on caspase-dependent cleavage of hScrib. As shown in Fig. 11, hScrib expression level in cells transfected with E6

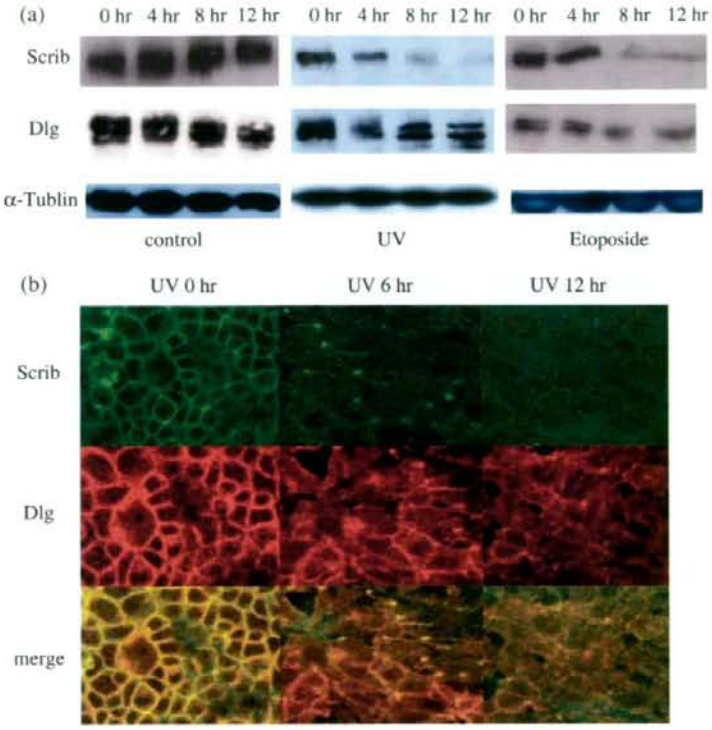

Figure 5 Loss of hScrib expression is earlier event in progressive apoptosis than that of hDlg. Expression of human homologues of *Drosophila* neoplastic tumor suppressor proteins, hScrib and hDlg, was analyzed by the Western blotting (a) and immunofluorescence staining (b) with anti-hScrib and anti-hDlg antibodies during progression of apoptosis. Both of assays indicate that hScrib is targeted by proteolysis earlier than hDlg in the progression of apoptosis induced by UV irradiation.

expression vector was lower than that in cells transfected with control vector, which is consistent with the previous report (Nakagawa & Huibregtse 2000). After induction of apoptosis, caspase-dependent cleavage of hScrib was more evident in cells transfected with control vector comparing with that in cells transfected with E6 expression vector (Fig. 11). The p220 hScrib was not observed in cells transfected with control vector and in those transfected with E6 expression vector after 24 h of UV irradiation, suggesting the possibility that E6 protein expression partially inhibit caspase-dependent cleavage of hScrib.

Discussion

Tissue homeostasis is kept in normal epithelial cells under the surveillance of programmed cell death mechanism (Igney & Krammer 2002). Over-proliferated or over-damaged cells are eliminated by the self-destruction mechanism called apoptosis (Steller 1995; Thompson 1995; Song & Steller 1999). Disruption of intrinsic cell–cell contact is a critical step in the process of apoptosis (Rosenblatt *et al.* 2001). A proteolytic cascade mediated by the caspases family of cysteine proteinases, which specifically cleave target proteins after aspartate residues, has a central role in cell death machinery (Brancolini *et al.* 1997). A number of proteins localized at the adherens and tight junctions have been reported to be targeted by caspases, including E-cadherin, β-catenin, FAK, PAK2, fodrin, plakoglobin, hDlg, focal adhesion kinase, ZO-1, ZO-2, occludin, MAGI-1 and MAGI-2 (Rudel & Bokoch 1997; Wen *et al.* 1997; Janicke *et al.* 1998; Levkau *et al.* 1998; Steinhusen *et al.* 2000, 2001; Bojarski *et al.* 2004; Gregorc *et al.* 2005, 2007; Ivanova *et al.* 2007). We have identified that hScrib is targeted for cleavage by executioner caspase activated by death ligands TNF-α and FAS ligands and UV irradiation. These data indicate that caspase-dependent cleavage of hScrib is a general event in apoptosis.

hScrib is human homologue of *Drosophila* tumor suppressor protein Scribble (Nakagawa & Huibregtse 2000). In *Drosophila*, three tumor suppressor genes (TSGs) *lgl*, *dlg* and *scrib* are categorized as neoplastic TSGs, in which mutation causes loss of apico-basolateral cellular polarity and tissue architecture and simultaneously induces extensive over proliferation in epithelia and neuroblasts (Bilder *et al.*

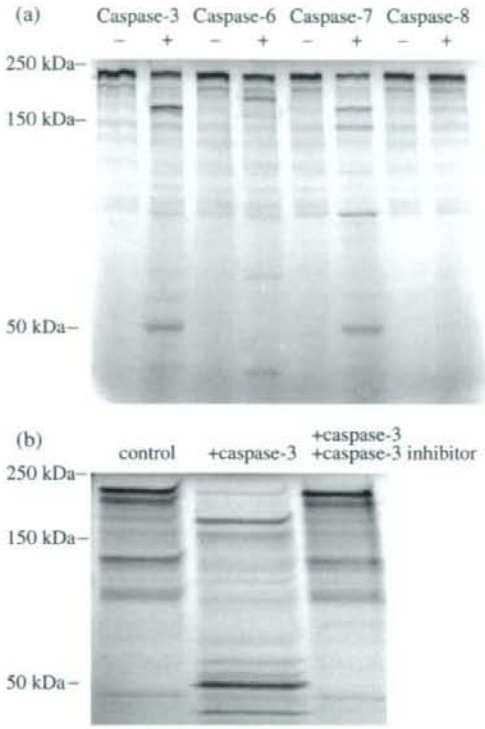

Figure 6 *In vitro* cleavage of hScrib with the executioner caspases. (a) *In vitro* translated [^{35}S] methione-labeled hScrib was incubated with recombinant caspase-3, caspase-6, caspase-7 and caspase-8 as described in the Materials and methods. Cleavage of hScrib by the executioner caspases was confirmed by the SDS electrophoresis and autoradiography. (b) The *in vitro* cleavage of hScrib by caspase-3 was completely repressed by the presence of caspase-3 inhibitor.

2000; Bilder 2003, 2004; Humbert *et al.* 2003; Hariharan & Bilder 2006). The *scrib* mutant clones proliferate, but these excess cells are eliminated by JNK-dependent apoptosis (Brumby & Richardson 2003; Pagliarini & Xu 2003; Tapon 2003). Loss of *scrib* mutation in activated Ras-expressing cells disrupted the epithelial structure of the eye imaginal disc and led to progressive invasion into neighboring structure (Pagliarini & Xu 2003). These data suggest the possibility that disruption of tissue polarity by loss of hScrib is involved in human carcinogenesis in concert with activated expression of oncogenic Ras. hScrib has been shown to be a functional homologue of the *Drosophila* Scribble (Dow *et al.* 2003). hScrib can rescue loss of polarity and inhibit tumorous overgrowth of *scrib* mutant *Drosophila* (Dow *et al.* 2003). Mammalian Scribble was shown to have crucial role in promotion of cell polarity in migrating astrocyte and epithelial cells (Osmani *et al.* 2006; Dow *et al.* 2007).

hScrib localizes at the adherens junction in normal epithelial cells and its expression is down-regulated in the precursor lesions and invasive cancers in the uterine cervix and colon (Nakagawa *et al.* 2004; Gardiol *et al.* 2006). Loss of hScrib expression was observed at the early stage of apoptosis identified by the positive TUNEL signal. hDlg is human homologue of *Drosophila* neoplastic tumor suppressor protein Discs large and is targeted for ubiquitin-mediated degradation by the high-risk HPV E6 protein (Gardiol *et al.* 1999). We analyzed loss of expression of these human homologues of *Drosophila* neoplastic tumor suppressor proteins during apoptosis and found that loss of hScrib expression is earlier event than that of hDlg. These data indicate that proper expression of hScrib is essential for construction of adherens junction and elimination of hScrib expression is also crucial for the disruption of junctional protein complex in damaged cells during apoptosis.

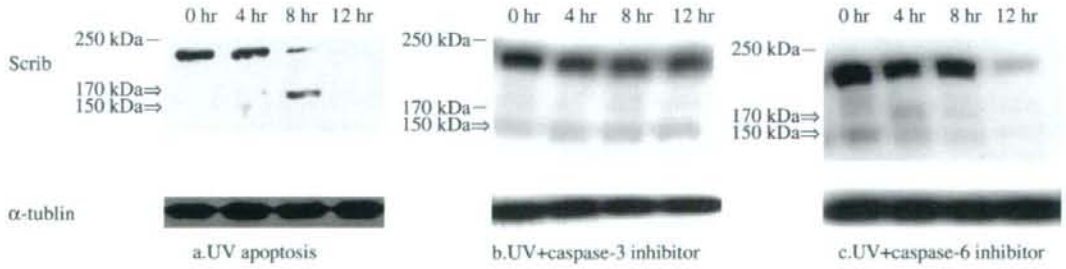

Figure 7 *In vivo* cleavage of hScrib by caspase-3 and caspase-6. The hScrib expression was lost by the irradiation of UV. The lost of hScrib expression after the apoptosis induction was inhibited by the presence of the inhibitor of executioner caspases, especially by the caspase-3 inhibitor. Note that generation of p170 hScrib was repressed by the caspase-3 inhibitor, but not by the caspase-6 inhibitor.

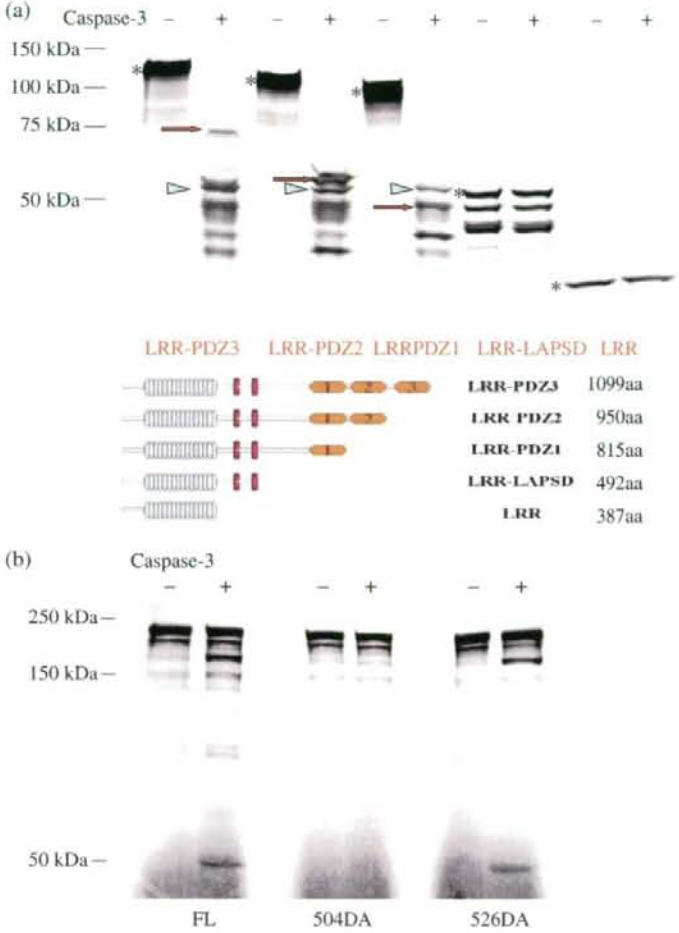

Figure 8 Analysis of cleavage site of hScrib by the caspase-3. (a) *In vitro* translated [^{35}S]-methione-labeled hScrib deletion mutants were incubated in the presence of recombinant caspases-3. The Scheme of hScrib C-terminal deletion mutants is shown in Fig. 8a. Human Scrib mutants, LRR–PDZ3, LRR–PDZ2 and LRR–PDZ1 were cleaved by recombinant caspase-3, whereas LRR–LAPSD and LRR were not susceptible for cleavage by caspase-3. Note that the protein band with same molecular weight (marked by the blue arrow head), which is considered to be the N-terminal part of proteins cleaved by caspase-3, is seen in cleaved LRR–PDZ3, LRR–PDZ2 and LRR–PDZ1 (Fig. 8a). The full-length translated hScrib mutants were indicated by the asterisk. Several fragments with much smaller sizes are seen for translated hScrib deletion mutants, especially for LRR–LAPSD. The protein bands, which are considered to be the C-terminal part of LRR–PDZ3, LRR–PDZ2 and LRR–PDZ1 hScrib mutants cleaved by caspase-3 are indicated by the red arrows. (b) Wild-type hScrib and Alanine substitution hScrib mutants of Asp 504 (D504A) and Asp526 (D526A) were tested for *in vitro* cleavage in the presence of recombinant caspases-3. Human Scrib D504A mutant is resistant to caspase-3 dependent cleavage.

We screened hScrib amino acids sequence for the potential cleavage site by caspase and found two D-X-X-D sequences (D_{1068}-V-R-D_{1071} and D_{1131}-P-T-D_{1134}), which are typical caspase-3 recognition sequences (Talanian *et al.* 1997). None of single amino acid substitution of these four Asp residues rendered hScrib resistant for caspase-dependent cleavage (K. S. and S. N. unpublished data). hScrib is a member of LAP (LRRs and PDZ domains) proteins. It has 16 canonical LRRs at the N-terminal region and four copies of the PDZ domain in its C-terminus (Santoni *et al.* 2002). Between these structures lies a 38-amino acid LRR-like domain called LAPSD-a. A second conserved sequence specific to LAP proteins and unrelated to LRR motifs between LRRs and PDZ domains resides at the downstream of LAPSD-a and is named as LAPSD-b. We investigated the region responsible for caspase-dependent cleavage by using deletion mutants of hScrib and found that PDZ domains are not targeted for cleavage by caspase-3 and that the

Figure 9 GFP-fused wild-type hScrib and hScrib D504 mutant were transfected in to MDCK cells. Apoptosis was induced with UV irradiation 48 h post-transfection. Cells were analyzed for the immunofluorescence staining of E-cadherin. Hoechst staining was carried out for the analysis of nuclear fragmentation. The expression of hScrib and E-cadherin was lost in the wild-type hScrib transfected cells (arrow), which show the fragmented nucleus, after induction of apoptosis. Note that expression of E-cadherin is intact as a control in cells transfected with hScrib D504A mutant (arrow), which is resistant for caspase-dependent cleavage, whereas nucleus shows typically apoptotic signal with condensed fragmentation.

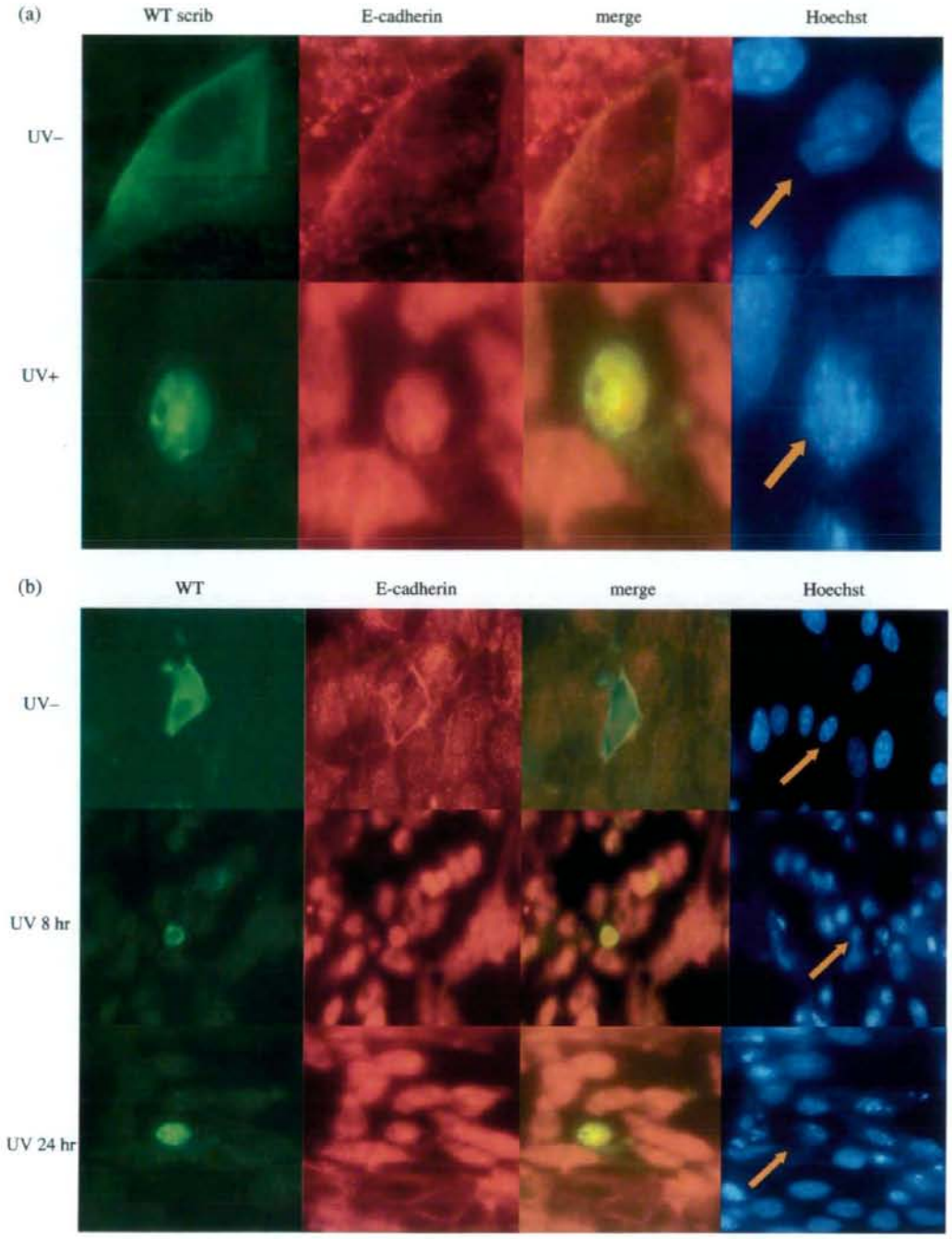

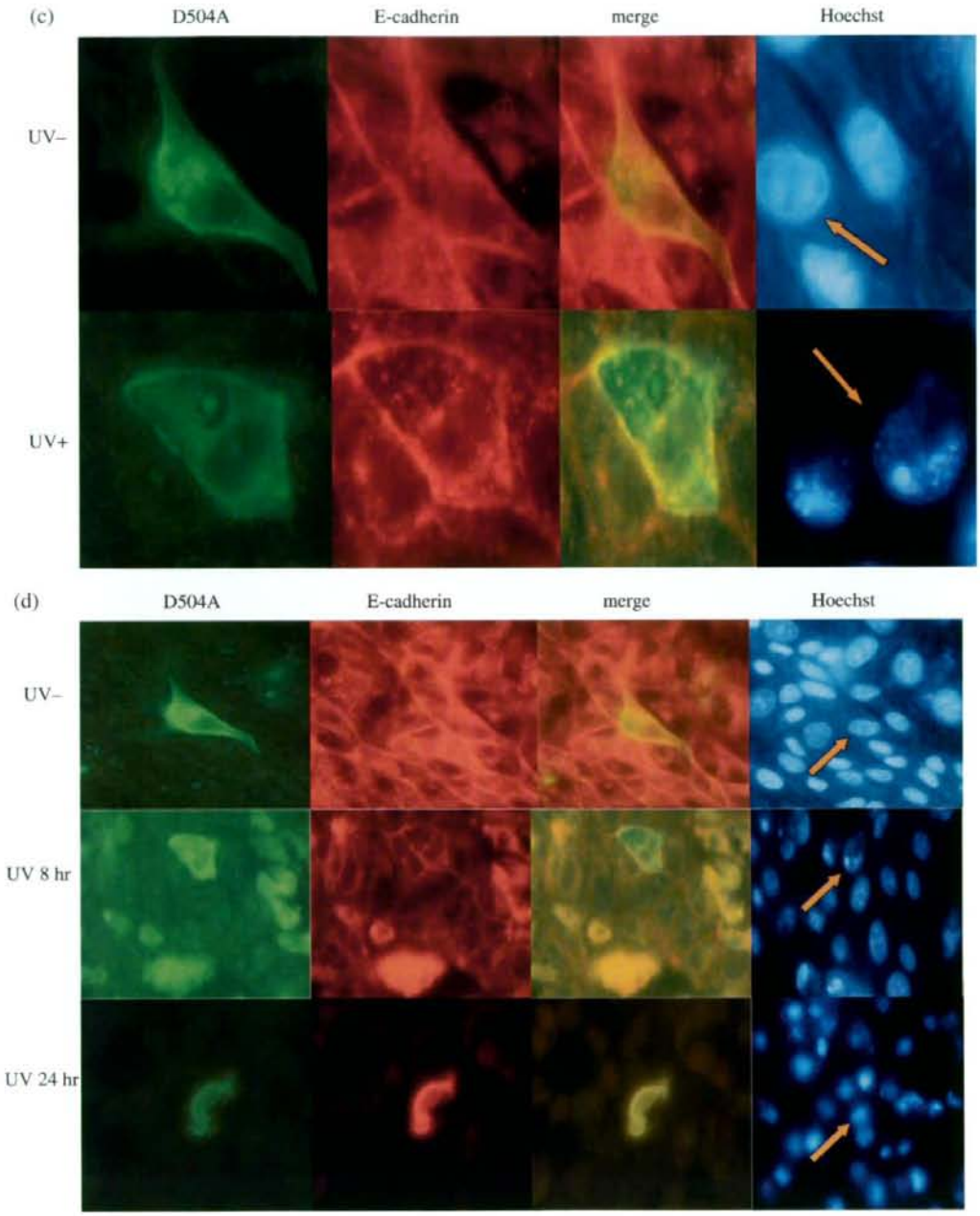

Figure 9 *Continued*

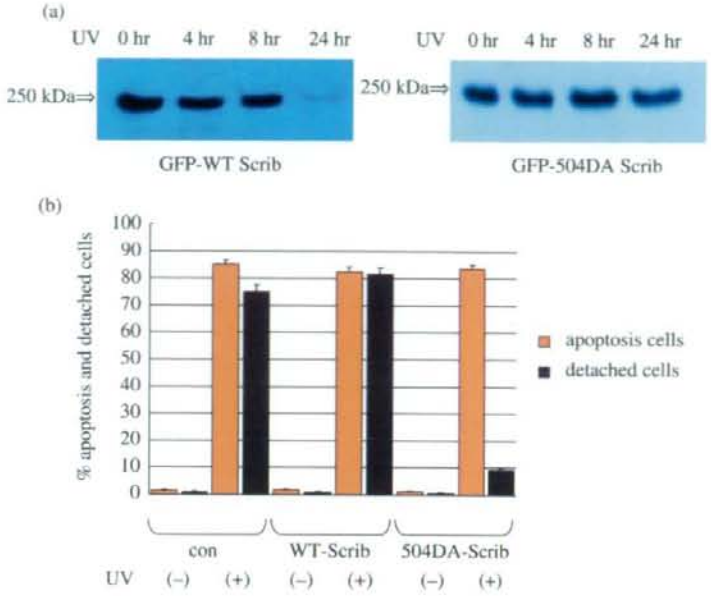

Figure 10 Human Scrib D504A mutant is resistant to caspase-dependent cleavage induced by apoptosis. (a) Immunoblotting analysis confirmed that over-expressed GFP–hScrib D504A mutant is resistant to caspase-dependent cleavage activated by apoptosis induction with UV irradiation. (b) To quantitate the effect of WT and Asp504Ala hScrib mutant on apoptosis induction and cellular detachment, 300 MDCK cells transfected with control vector, GFP–WT hScrib vector, or GFP–hScrib D504A mutant vector were analyzed for apoptosis signals and cellular detachment by Hoechst staining and immunofluorescence analysis of E-cadherin, respectively. The ratio of apoptosis positive cells and detached cells as evidenced by loss of E-cadherin in 300 cells transfected with each vector was analyzed for absence and presence of UV irradiation and shown as histograms.

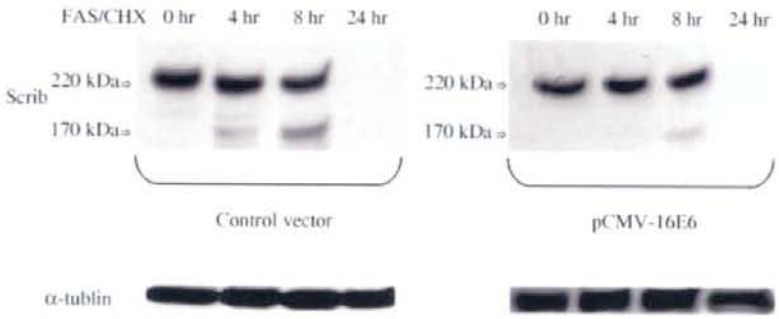

Figure 11 The effect of HPV E6 on the caspase-dependent cleavage of hScrib. Apoptosis was induced by UV irradiation at 48 h post-transfection of control vector or E6 expression vector. Prior the apoptosis induction, hScrib expression level was lower in cells transfected with E6 expression vector. After induction of apoptosis, caspase-dependent cleavage of hScrib was more obvious in cells transfected with control vector as evidenced by the generation of p170 at 4 h post-UV irradiation comparing with that in cells transfected with E6 expression vector. Note that p170 was not observed in cells transfected with E6 vector after 4 h of UV irradiation.

amino acids sequence between LRRs and PDZ domain 1 is potential caspase-dependent cleavage site. The site-specific mapping of a critical amino acid for the caspase-dependent cleavage of hScrib with mutagenesis showed that first ASP residue (amino acid 504) in the region between LAPSD-b and PDZ domain 1 is targeted for cleavage by caspase-3. hScrib N-terminal region containing LRRs, LAPSD-a and LAPSD-b ($hScrib_{1-724}$ and $hScrib_{1-518}$) is reported to localize at the basolateral epithelial membrane (Navarro *et al.* 2005). Our previous study showed that $hScrib_{1-495}$ localizes in the cytoplasm, not at the membrane (Nagasaka *et al.* 2006). It is possible that the cleaved hScrib at amino acid 504 by caspase-3 ($hScrib_{1-504}$) does not target the basolateral membrane. For *Drosophila* Scribble, multi-step localization through LRRs and PDZ domains are necessary for establishment of cortical polarity (Albertson *et al.* 2004; Zeitler *et al.* 2004). hScrib has been shown to be involved in polarity

control in migrating cells by interacting βPIX exchange factor and APC (Audebert *et al.* 2004; Takizawa *et al.* 2006; Dow *et al.* 2007). hScrib have been reported to interact with ZO-2 and zyxin-related proteins, Lipoma Preferred Partner (LPP) protein and TRIP6, at epithelial cellular junctions through its PDZ domains (Metais *et al.* 2005; Petit *et al.* 2005a,b). The caspase-3 dependent cleavage of hScrib at amino acid 504 might disrupt these protein complexes formations at the epithelial cellular junctions through its PDZ domains. The resistance to distraction of adherens junction in the apoptosis-induced epithelial cells transfected with hScrib D504A mutant indicates that caspase-3 dependent cleavage of hScrib is a critical step for elimination of dying cell from normal cells. Our analysis of the effect of E6 expression on the caspase-dependent cleavage of hScrib indicated the possibility that E6 partially inhibit the cleavage. These data suggest the possibility that E6 render some cellular fractions of hScrib resistant to the caspase-dependent cleavage. Further investigations would be required to show comprehensive mechanisms underlying the partial inhibition of caspase-dependent cleavage of hScrib by E6 protein.

In summary, we found that hScrib, which has a fundamental role in tissue polarity architecture, is a novel death substrate targeted by caspase-3. The caspase-dependent cleavage of human homologues of *Drosophila* neoplastic tumor suppressors, hScrib and hDlg, is considered to be an essential step in the elimination of apoptotic cells from the surrounding healthy cells.

Experimental procedures

Tissue culture and apoptosis induction

Human HaCat, CaCo-2 cells and Hela cells were grown in DMEM supplemented with 10% fetal bovine serum. Before induction of apoptosis, cells were plated onto 10-cm dishes and allowed to reach to the confluency. Apoptosis was induced by irradiating UV light (0.24 J) or adding 200 nM etoposide (Sigma, St Louis, MO), 500 ng/mL anti-Fas (MBL, Nagoya, Japan), 100 μg/mL Cycloheximide (CHX) (Sigma) and/or 2000 U/mL TNF (Relia Tech GmbH, Braunschweig, Germany) into the medium. In an additional experiment using caspase inhibitors, 50 μM Z-DEVD-FMK (R&D systems, Minneapolis, MN or Ac-VEID-CHO (Biomol, Pennsylvania, PA) was added into the medium and apoptosis was induced as described above.

Western blotting

Following apoptosis induction, cells were harvested at the indicated hours after induction of apoptosis. The protein concentration of the samples was equalized and samples were analyzed by electrophoresis on 6% SDS PAGE. Levels of hScrib and hDlg protein were determined by Western blotting using ECL advance Western blotting Detection Kit (GE Healthcare Bio-science, Piscataway, NJ) according to the manufacture's instructions. The expression of hScrib was detected using the anti-hScrib goat monoclonal antibody (Santa Cruz Biotechnology, Santa Cruz, CA) or the anti-hScrib polyclonal antibody raised in rabbit against its PDZ domains as an antigen. The expression of hDlg was detected using the anti-hDlg mouse monoclonal antibody. (Santa Cruz Biotechnology). The expression of Lamin B1 was detected using the anti-Lamin B1 mouse monoclonal antibody. (Santa Cruz Biotechnology). The expression of procaspase-3 was detected using the anti-caspase-3 mouse monoclonal antibody. (Santa Cruz Biotechnology). The expression of GFP–Scrib was detected using the anti-GFP mouse monoclonal antibody (Zymed, San Francisco, CA).

Fluorescence microscopy

HaCaT and CaCo-2 cells were grown overnight on cover slips before induction of apoptosis. Cells were washed with phosphate-buffered saline (PBS) and fixed with 3.7% paraformaldehyde in PBS for 30 min at the times indicated, followed by permeabilization with 0.2%(v/v) Triton X-100 in PBS for 5 min. After extensive washing with 1% BSA–PBS, the cells were incubated with anti-hScrib antibody diluted 1 : 400, and anti-hDlg diluted 1 : 100 in PBS for 60 min. Following an additional round of wash with PBS containing 1% BSA, cells were incubated with donkey anti-goat and rabbit anti-mouse Allexa488 and 568 conjugated antibodies (Invitrogen, Eugene, OR) for 60 min. Expression of protein was investigated under the confocal fluorescence microscopy.

To analyze apoptosis signal, cells were incubated with Hoeshst33342 (Sigma) for 7 min, washed in PBS with 1% BSA, and then mounted on slides.

MDCK cells were transfected with GFP-tagged human scribble constructs, using the PolyFect Transfection Reagent (Qiagen, Hiden, Germany) or Effectene Transfection Reagent (Qiagen) according to manufacturer's instructions. To see the effect of HPV E6 on the caspase-dependent cleavage of hScrib during apoptosis, 293T cells were transfected with HPV E6 expression plasmid (Nakagawa & Huibregtse 2000).

Apoptosis is induced 48 h post-transfection with UV irradiation. At the indicated hours, cells were collected and treated as described above or stained with anti-E-cadherin antibody (BD Transduction Laboratories, Franklin Lakes, NJ) and Alexa568 conjugated anti-mouse antibodies (Molecular Probes, Eugene, OR). In addition, Hoeshst33342 was used to stain the nuclei. Morphological changes of cells induced of apoptosis were monitored using confocal fluorescence microscopy. To quantify the effect of WT hScrib or hScrib mutant D504A on cellular detachment during apoptosis, number of cells showing apoptosis (fragmentation of nucleus, and shrinkage of cytoplasm) and cellular detachment (loss of E-cadherin) were analyzed in 300 MDCK cells transfected with control vector, GFP–WT hScrib, or GFP–hScrib D504A mutant.

In vitro translation of proteins

Proteins were expressed using the Promega TNT coupled transcription-translation Rabbit-Reticulocyte lysate system (Promega,